Metabolic pathways promoting intrahepatic fatty acid accumulation in methionine and choline deficiency: implications for the pathogenesis of steatohepatitis

David P. Macfarlane, Xiantong Zou, Ruth Andrew, Nicholas M. Morton, Dawn E. W. Livingstone, Rebecca L. Aucott, Moffat J. Nyirenda, John P. Iredale and Brian R. Walker

Am J Physiol Endocrinol Metab 300:E402-E409, 2011. First published 30 November 2010; doi:10.1152/ajpendo.00331.2010

Am J Physiol Endocrinol Metab 300: E402–E409, 2011.
First published November 30, 2010; doi:10.1152/ajpendo.00331.2010.

Metabolic pathways promoting intrahepatic fatty acid accumulation in methionine and choline deficiency: implications for the pathogenesis of steatohepatitis

David P. Macfarlane,[1] Xiantong Zou,[1] Ruth Andrew,[1] Nicholas M. Morton,[2] Dawn E. W. Livingstone,[1] Rebecca L. Aucott,[3] Moffat J. Nyirenda,[1] John P. Iredale,[3] and Brian R. Walker[1]

[1]*University/BHF Centre for Cardiovascular Science, Endocrinology Unit,* [2]*University/BHF Centre for Cardiovascular Science, Molecular Metabolism Group, and* [3]*Univeristy/MRC Centre for Inflammation Research, Queen's Medical Research Institute, University of Edinburgh, Edinburgh, United Kingdom*

Submitted 2 June 2010; accepted in final form 29 November 2010

Macfarlane DP, Zou X, Andrew R, Morton NM, Livingstone DE, Aucott RL, Nyirenda MJ, Iredale JP, Walker BR. Metabolic pathways promoting intrahepatic fatty acid accumulation in methionine and choline deficiency: implications for the pathogenesis of steatohepatitis. *Am J Physiol Endocrinol Metab* 300: E402–E409, 2011. First published November 30, 2010; doi:10.1152/ajpendo.00331.2010.—The pathological mechanisms that distinguish simple steatosis from steatohepatitis (or NASH, with consequent risk of cirrhosis and hepatocellular cancer) remain incompletely defined. Whereas both a methionine- and choline-deficient diet (MCDD) and a choline-deficient diet (CDD) lead to hepatic triglyceride accumulation, MCDD alone is associated with hepatic insulin resistance and inflammation (steatohepatitis). We used metabolic tracer techniques, including stable isotope ([$^{13}C_4$]palmitate) dilution and mass isotopomer distribution analysis (MIDA) of [$^{13}C_2$]acetate, to define differences in intrahepatic fatty acid metabolism that could explain the contrasting effect of MCDD and CDD on NASH in C57Bl6 mice. Compared with control-supplemented (CS) diet, liver triglyceride pool sizes were similarly elevated in CDD and MCDD groups (24.37 ± 2.4, 45.94 ± 3.9, and 43.30 ± 3.5 μmol/liver for CS, CDD, and MCDD, respectively), but intrahepatic neutrophil infiltration and plasma alanine aminotransferase (31 ± 3, 48 ± 4, 231 ± 79 U/l, $P < 0.05$) were elevated only in MCDD mice. However, despite loss of peripheral fat in MCDD mice, neither the rate of appearance of palmitate (27.2 ± 3.5, 26.3 ± 2.3, and 28.3 ± 3.5 $\mu mol \cdot kg^{-1} \cdot min^{-1}$) nor the contribution of circulating fatty acids to the liver triglyceride pool differed between groups. Unlike CDD, MCDD had a defect in hepatic triglyceride export that was confirmed using intravenous tyloxapol (142 ± 21, 122 ± 15, and 80 ± 7 $mg \cdot kg^{-1} \cdot h^{-1}$, $P < 0.05$). Moreover, hepatic de novo lipogenesis was significantly elevated in the MCDD group only (1.4 ± 0.3, 2.3 ± 0.4, and 3.4 ± 0.4 μmol/day, $P < 0.01$). These findings suggest that important alterations in hepatic fatty acid metabolism may promote the development of steatohepatitis. Similar mechanisms may predispose to hepatocyte damage in human NASH.

nonalcoholic fatty liver disease; steatohepatitis; free fatty acids; de novo lipogenesis; methionine- and choline-deficient diet; choline-deficient diet

NONALCOHOLIC FATTY LIVER DISEASE (NAFLD) is an increasingly recognized entity encompassing a spectrum of severity ranging from uncomplicated triglyceride accumulation (or steatosis) to inflammation (steatohepatitis), fibrosis, cirrhosis, and hepatocellular carcinoma (31). The mechanisms underlying susceptibility to progressive liver disease in NAFLD remain poorly understood. Importantly, it is not known whether specific changes in hepatic triglyceride handling leading to the accumulation of intracellular fatty acids predispose to hepatocyte damage and the development of nonalcoholic steatohepatitis (NASH).

Broadly speaking, the accumulation of hepatic triglyceride can be considered an imbalance between the supply of free fatty acids (FFAs) from both plasma and intrahepatic de novo lipogenesis (DNL) and their removal by either fatty acid oxidation or export in very low-density lipoprotein (VLDL). Studies in humans suggest that both increased release of FFAs from extrahepatic tissues and increased DNL contribute to the accumulation of liver triglyceride in NAFLD (8–10). Such abnormalities of fatty acid metabolism may play a role not only in the insulin resistance associated with NAFLD but also in promoting hepatic inflammation. In addition to influencing rates of hepatic gluconeogenesis and VLDL export (6, 25), FFAs are inherently toxic to hepatocytes (30), e.g., activating the proinflammatory cytokine nuclear transcription factor-κB (12, 19) and upregulating mediators of apoptosis (11). A toxic role for FFAs in the liver is supported by the observation that inhibiting diacylglycerol acyltransferase 2, the final enzyme in the pathway esterifying fatty acids to triglycerides, promotes steatohepatitis and liver fibrosis in mice despite reducing intrahepatic triglycerides (45).

In humans, practical limitations mean that only the broadest association can be made between hepatic triglyceride/fatty acid handling and NASH. In contrast, the mechanisms underlying susceptibility to steatohepatitis and fibrosis mediated by fatty acids can be defined by studies in animal models with contrasting susceptibility to NASH. Feeding rodents diets deficient in choline and/or methionine reliably leads to the accumulation of intrahepatic triglyceride (15, 32), but there are contrasting consequences for liver inflammation. A methionine- and choline-deficient diet (MCDD) causes steatohepatitis and hepatic insulin resistance (24, 37, 39), although peripheral insulin sensitivity is improved due to significant weight loss (38). In contrast, a simple choline-deficient diet (CDD) leads to steatosis without significant inflammation and is associated with improved hepatic and peripheral insulin sensitivity without weight loss following a high-fat diet (36). These diets provide readily tractable models to define the differences in hepatic fatty acid metabolism that underlie susceptibility to NASH as opposed to simple steatosis.

Impaired VLDL export was previously thought to be the dominant mechanism for the accumulation of liver fat in both CDD and MCDD models (29). More recent ex vivo studies

Address for reprint requests and other correspondence: B. R. Walker, Univ. of Edinburgh, Endocrinology Unit, Centre for Cardiovascular Science, Queen's Medical Research Institute, 47 Little France Crescent, Edinburgh EH16 4TJ, UK (e-mail: B.Walker@ed.ac.uk).

have shown that VLDL export may not be decreased in CDD mice (22), whereas alterations in gene expression support the hypothesis that a primary increase in fatty acid esterification protects CDD mice against the toxic effects of intrahepatic fatty acids (36). Moreover, weight loss in MCDD but not CDD mice suggests that increased flux of potentially toxic FFAs from the periphery to the liver may occur only with MCDD. However, these inferences concerning fatty acid metabolism in MCDD and CDD mice are drawn indirectly from ex vivo measurements. We have characterized fatty acid metabolism in detail in vivo using stable isotope tracers in mice fed CDD and MCDD and identified pathways that could explain contrasting propensity to hepatocyte damage and steatohepatitis in these models, observations with implications for understanding the pathogenesis of human NASH.

MATERIALS AND METHODS

Materials

Stable isotope-labeled tracers were from Cambridge Isotopes (Andover, MA), and all other chemicals were from Sigma (Poole, UK) unless otherwise stated. Solvents were glass-distilled HPLC grade (Rathburn, Walkerburn, UK). Human albumin solution (20%) was from the Scottish National Blood Transfusion Service (Lothian, UK).

Animals and Procedures

All experiments were carried out under a UK Home Office animal license. Twelve-week-old male C57BL/6J mice (Harlan, Bicester, UK) were maintained under controlled conditions of light and temperature. Following a 2-wk period of acclimatization, mice were offered either control (choline and methionine supplemented; CS) chow, CDD, or MCDD (Dyets, Bethlehem, PA) for 2 wk. The dietary compositions are shown in Table 1; to prevent unavoidable contamination of choline and methionine from protein, the protein content was replaced by pure L-amino acids (32).

Fatty Acid Flux Studies

To quantify FFA turnover by stable isotope dilution, 1,2,3,4-[$^{13}C_4$]palmitate was infused intravenously (n = 12–15 mice/group), and tracer enrichment of the palmitate pool in liver, adipose tissue, and plasma was measured by gas chromatography-mass spectrometry (GC-MS) (1).

Jugular venous cannulae were inserted under general anesthesia (intraperitoneal medetomidine and ketamine) on *day 10* of dietary manipulations, and mice were allowed 4 days to recover prior to tracer infusions. [$^{13}C_4$]palmitate was prepared by dissolving its potassium salt in saline and complexing with 20% wt/vol albumin solution at 40°C. In initial studies, a stock solution was diluted so that infusion at 5 μl/min provided 0.271 $\mu mol \cdot kg^{-1} \cdot min^{-1}$ tracer (1, 20). Following preliminary analysis, the concentration was later increased so that the infusion delivered 0.542 $\mu mol \cdot kg^{-1} \cdot min^{-1}$ to increase tissue enrichment. Calculated kinetic results were similar in both groups, so data were combined for statistical analysis. Following a 4-h fast, the tracer infusion was commenced using a Harvard apparatus syringe pump (World Precision Instruments, Stevenage, UK) for 180 min (20). Animals were euthanized by decapitation within 60 s of being disturbed, and trunk blood was collected on wet ice. Plasma was stored at −80°C. Liver and adipose depots were immediately harvested, weighed, and snap-frozen on dry ice. Palmitate and its tracer were quantified by GC-MS and triglycerides (TG) by spectrophotometric assay as detailed below.

Table 1. *Composition of rodent diets*

	CS	CDD	MCDD
Kcal/g	4.3	4.3	4.3
Kcal%			
Protein (as L-amino acids)	15	15	15
Carbohydrate	55	55	55
Fat	30	30	30
Choline bitartate, g/kg	14.48	0	0
L-Methionine, g/kg	1.7	1.7	0

CS, control diet; CDD, choline-deficient diet; MCDD, methionine- and choline-deficient diet. Diets were purchased from Dyets (Bethlehem, PA), with the following manufacturers' reference codes: CS, 518574; CDD, 518753; MCDD, 518810. All diets contained 50 g/kg corn oil (source of polyunsaturated fat) and 100 g/kg Primex (hydrogenated vegetable oil) as lipid sources. Carbohydrate was composed of corn starch, dextrin, cellulose, and sucrose, with sucrose differing marginally between the groups (392, 406, and 408 g/kg for the CS, CDD, and MCDD, respectively).

Kinetic Calculations

Assuming steady-state conditions after 180 min of infusion (1), the rate of appearance (R_a) of palmitate in plasma was calculated using *Eq. 1*:

$$R_a\left(\mu mol \cdot kg^{-1} \cdot min^{-1}\right) = F/IE, \quad (1)$$

where F is the isotope infusion rate ($\mu mol \cdot kg^{-1} \cdot min^{-1}$) and IE is the isotopic enrichment (the tracer/tracee ratio).

An index of the contribution of circulating FFAs to TG pools in tissues and plasma was estimated using *Eq. 2* (1, 8, 20):

$$\text{Fraction of TG palmitate derived from plasma FFA} = \text{IE of } [^{13}C_4] \text{ palmitate in TG} / \text{IE of } [^{13}C_4] \text{ palmitate in plasma.} \quad (2)$$

The absolute contribution of circulating palmitate to tissue or plasma TGs was calculated by correcting for the TG pool size using *Eq. 3*:

$$\text{Absolute palmitate uptake} = \text{fraction of TG palmitate derived from plasma} \times \text{TG pool size,} \quad (3)$$

where tissue and plasma TG pool sizes were calculated by multiplying TG concentration by tissue weight [assuming adipose tissue to be composed of pure TG of molecular weight 861 (14)] or estimated plasma volume [3.5% of body weight (18)], respectively.

DNL Studies

To assess DNL, in other groups of mice (n = 8/group), [$^{13}C_2$]acetate was added to diets for 5 days before euthanization and incorporation of ^{13}C into TG assessed in liver and plasma using mass isotopomer distribution analysis (MIDA) after analysis of TG-derived palmitate and its labeled isotopomers by GC-MS (1, 17). Mice were housed individually and fed diets as described above in a paste (225 g of powdered chow as described above with 45 ml of water) packed into 50-ml plastic tubes to facilitate weighing of food intake. For the final 5 days, labeled [$^{13}C_2$]acetate (4.5 g) was added to the water before preparation of the paste. Tissues were collected as described above. Snap-frozen livers from these mice were also used for real-time PCR studies.

MIDA

GC-MS was used to determine the pattern of incorporation of [$^{13}C_2$]acetate into newly synthesized hepatic TG FFAs using the method of Chinkes et al. (7), and the fractional synthesis rate, i.e., the fraction of the liver TG-palmitate pool synthesized per unit of time, was calculated using *Eq. 4*:

$$FSR = \left[E_b(t2) - E_b(t1)\right] / \left[(t2 - t1) \times EF\right], \quad (4)$$

where FSR is the fractional synthesis rate, E_b is the singly labeled product (palmitate) enrichment at time points $t2$ and $t1$ in moles percent excess (MPE), and EF is the calculated precursor (acetyl-

CoA) enrichment converted into the same units of singly labeled product enrichment using *Eq. 5* (7). Baseline enrichment (*t*1) was determined from the livers from the VLDL export experiment.

$$EF = n \times p \times (1 - p)^{n-1}, \quad (5)$$

where p is the calculated precursor enrichment in MPE and n is the maximum number of acetyl-CoA molecules that could appear in palmitate (i.e., 8), as described in detail elsewhere (7).

The absolute synthesis rate was calculated by multiplying the FSR by the size of the TG pool (in μmol), estimated as described above. The same calculations were used to calculate the export of newly synthesised fatty acids into the plasma TG pool.

Hepatic TG Export Studies

In additional mice (n = 7–8/group), following a 4-h fast, hepatic VLDL export was assessed by measuring the rate of accumulation of TG (quantified by spectrophotometry) in plasma from serial tail nicks taken at 0, 30, 60, 120, and 180 min following administration of tyloxapol (Triton W1339) by tail vein injection (500 mg/kg, 15% vol/vol in normal saline) (26). *Eq. 6* converted the R_a per plasma volume into whole body R_a, and plasma volume was estimated as 3.5% of body weight (18).

$$\text{TG export}\left(\text{mg}\cdot\text{kg}^{-1}\cdot\text{h}^{-1}\right) = \left[\text{slope of line}\left(\text{mg}\cdot\text{dl}^{-1}\cdot\text{min}^{-1}\right) \times \text{estimated plasma volume}\left(\text{dl}\right)\right] / \left[\text{weight}\left(\text{kg}\right) \times 60\right]. \quad (6)$$

Hepatic Inflammation Studies

In an additional study (n = 10/group), livers were fixed in 10% formalin for immunohistochemical analysis after 2 wk of dietary interventions, as described above. In addition, fasting plasma samples from these mice were used for measurement of liver function tests and total plasma FFAs.

Biochemical Assays

Lipid extraction. Palmitate and its tracer were extracted from plasma (50 μl) containing heptadecanoic acid (5 μg) internal standard and derivatized to their methyl esters (33) prior to analysis by GC-MS. For analysis of TGs, plasma and tissue lipids were extracted using a modified Folch technique (13) with triheptadecanoic acid (5 μg) internal standard, and TGs were separated by solid-phase extraction using aminopropyl silica cartridges (100 mg; Bondelut Varian, Harbor City, CA), ensuring that the columns remained wetted between samples. TGs were hydrolyzed to their constituent FFAs and derivatized to their methyl esters using acidified methanol (2% vol/vol) sulphuric acid (34%) in methanol (18 h, 50°C) prior to extraction into hexane (4).

GC-MS analysis of palmitate. GC-MS analysis was undertaken on a ThermoFinnigan Voyager gas chromatograph mass spectrometer with an Agilent HP-Innowax column (30 m, 0.320 mm, 0.5 μm) operated in electron impact ionization mode (70 eV). Source, interface, and injection temperatures were 200, 250, and 260°C, respectively. The column temperature was programmed from a 1.5-min hold at 50°C, with a 13°C/min ramp and a 1.5-min hold at 260°C. Fatty acid methyl esters derived from plasma FFA and TG pools were analyzed using selective ion monitoring of molecular ions with mass-to-charge ratios of 270, 272, 274, and 284, corresponding to [M + 0], [M + 2], and [M + 4] isotopomers of methyl palmitate and the methyl heptadecanoate internal standard, respectively. To avoid concentration-dependent effects of methyl palmitate on ionization, each sample was analyzed several times using a range of injection volumes, as described previously (34).

Enzymatic assays. Plasma and liver TGs were quantified enzymatically using a colorimetric assay (Infinity; ThermoTrace), as described previously (36). Plasma FFAs were measured in duplicate using a commercial kit (Wako, Fuggerstrabe, Germany), and liver function tests, including alanine aminotransferase and aspartate aminotransferase, were measured using commercial colorimetric kits (Randox Laboratories, Antrim, UK) adapted for use on a Cobras centrifugal analyzer (Roche Dignostics, Welwyn Garden City, UK).

Quantitative Real-Time PCR

Total hepatic mRNA was extracted using a Qiagen RNeasy extraction kit (Crawley, UK) per the manufacturer's instructions and quantified at λ260/280. Integrity was checked by agarose gel electrophoresis (n = 6–8/group). Complementary DNA was synthesized from 0.5 μg of mRNA following genomic DNA wipeout using the Qiagen reverse transcription kit. Quantification of hepatic gene transcription was performed by real-time PCR using the Roche (Burgess Hill, UK) lightcycler 480 system. Primers and probes were from the Roche UPL library. The relative amount of mRNA was derived from standard curves prepared from serial dilutions of complementary DNA, and transcript levels were normalized to mean values of TBP and β-actin as housekeeping genes.

Immunohistochemistry

Paraffin-embedded sections of liver were stained using an anti-granulocyte antibody (108413 rat anti-mouse GR1 antibody; Cambridge Biosciences, Cambridge, UK). Liver sections were dewaxed in xylene and rehydrated in alcohol, and endogenous peroxide activity was blocked by washing in 1% hydrogen peroxide solution. After washing in phosphate-buffered saline (PBS), slides were mounted in Shandon Sequenza racks (Thermo Fisher Scientific, Leics, UK). A

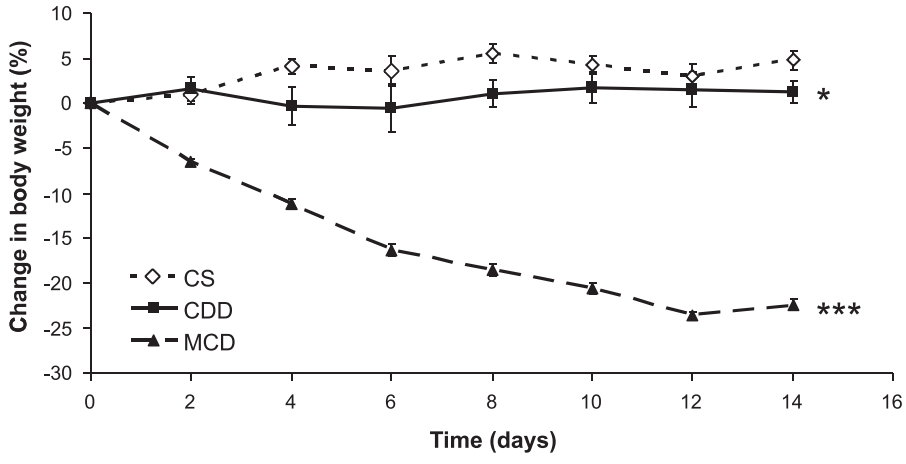

Fig. 1. Effect of methionine ± choline deficiency on body weight. Data points represent means ± SE; n = 8–30/group depending on time point. Final weights were analyzed by 1-way ANOVA with Tukey's post hoc comparison test. CS, control diet; CDD, choline-deficient diet; MCDD, methionine- and choline-deficient diet. *$P < 0.05$; ***$P < 0.001$.

Table 2. *Effect of choline ± methionine deficiency on liver weights and TGs, adipose depot weights, and food intake*

	CS	CDD	MCDD
Liver weight, %body weight	4.0 ± 0.1	4.7 ± 0.1***	3.8 ± 0.1†††
Liver TG pool, μmol/liver$	24.37 ± 2.4	45.94 ± 3.9***	43.30 ± 3.5***
Adipose depot weights, %body wt			
Subcutaneous$	1.5 ± 0.2	1.3 ± 0.1	0.7 ± 0.1***††
Epididymal$	1.6 ± 0.1	1.4 ± 0.1	0.4 ± 0.0***†††
Mesenteric§	0.3 ± 0.1	0.4 ± 0.1	0.1 ± 0.0*†††
Food intake, g·kg body wt^{-1}·day^{-1}§	127.9 ± 4.5	130.8 ± 2.8	104 ± 2.7***†††
Liver function tests§			
Bilirubin, μmol/l	4.9 ± 0.8	4.5 ± 0.7	5.3 ± 0.6
ALT, U/l	31 ± 3	48 ± 4	231 ± 79†*
AST, U/l	303 ± 86	224 ± 22	507 ± 90†

Data are means ± SE, analyzed by 1-way ANOVA with Tukey's post hoc tests where appropriate. TG, triglyceride; ALT, alanine aminotransferase; AST, aspartate aminotransferase. *$P < 0.05$, ***$P < 0.001$ vs. CS; †$P < 0.05$, ††$P < 0.01$, and †††$P < 0.001$ vs. CDD. Data were collected in different experiments and combined here, hence the varying numbers; $$n$ = 21–23/group, §n = 7–8/group. For all other variables, n = 28–30/group.

commercial avidin-biotin blocking kit (Vector Laboratories, Burlingame, CA) was used to block any background staining, and washing with PBS (×3) occurred between stages. Sections were blocked using normal rabbit serum (DAKO, Ely, UK) diluted 1:4 in PBS, with incubation occurring for 30 min at room temperature. Samples were then incubated with a 1-in-200 dilution (in rabbit serum) of the primary anti-granulocyte antibody (108413 rat anti-mouse GR1 antibody; Cambridge Biosciences) overnight at 4°C. After 0.1% Tween and PBS washes, sections were incubated for 60 min at room temperature, with a 1:300 dilution (in normal rabbit serum) of the secondary rabbit anti-rat antibody (DAKO) for 30 min at room temperature. Sections were incubated with three drops of the Vector RTU ABC reagent (30 min at room temperature) and anti-GR1 positive cells visualized using diaminobenzidine staining. Sections were counterstained in hemotoxylin (~15 s) and blued in Scott's tap water (~5 s) prior to dehydration through alcohol, clearing in xylene, and mounting in DPX mountant. Cell counts of neutrophils were undertaken in a blinded manner, averaging the number of cells in 40 representative high-power fields (×400) per liver section.

Statistical Analysis

Results are presented as means ± SE and were compared by one-way ANOVA with Tukey's post hoc multiple comparison test when appropriate.

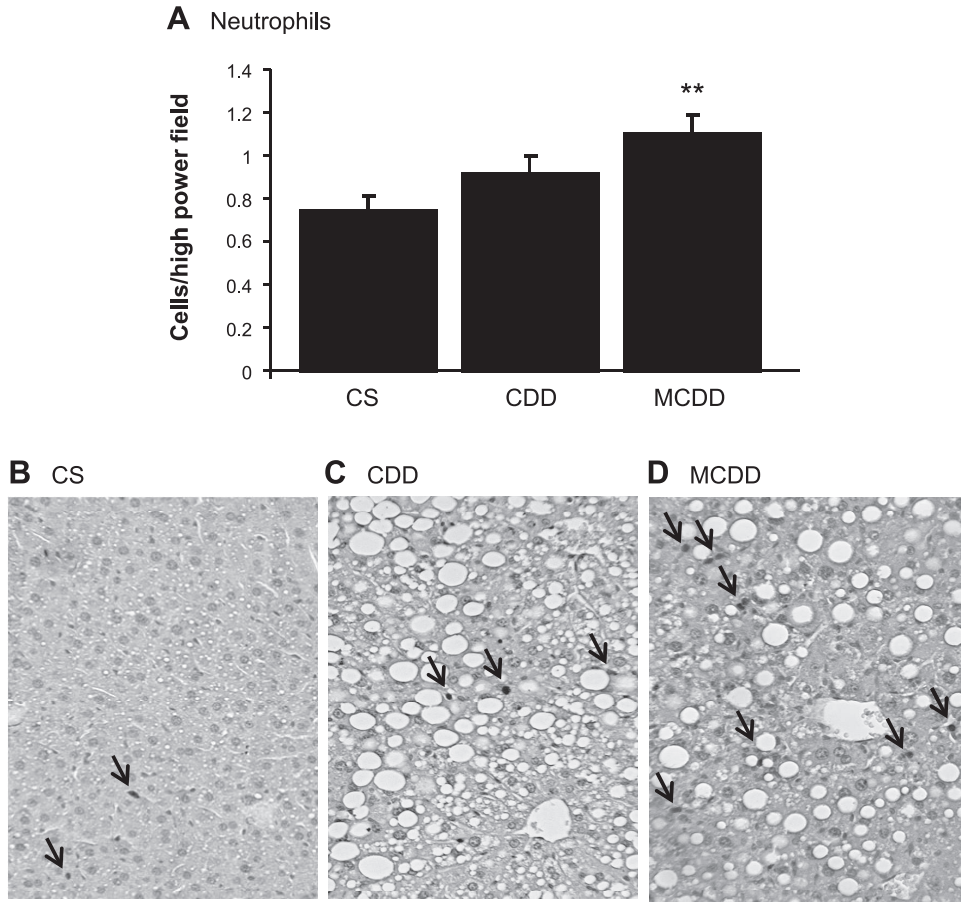

Fig. 2. Effects of methionine ± choline deficiency on liver inflammatory cell infiltration. Data are means ± SE for n = 10/group. Two weeks of MCDD but not CDD produced an increase in neutrophil staining. *A*: average cell counts of anti-GR1-positive staining cells per high-power fields; **$P < 0.05$. Exemplary GR1-positive staining cells in CS group (*B*), CDD (*C*), and MCDD (*D*). Original magnification, ×250. Arrows indicate immunopositive cells.

Table 3. *Effect of choline ± methionine deficiency on fatty acid flux measured by dilution of [$^{13}C_4$]palmitate tracer*

	CS	CDD	MCDD
R_a palmitate, μmol·kg^{-1}·min^{-1}	27.16 ± 3.46	26.25 ± 2.27	28.34 ± 3.46
Fractional contribution to liver TG pool, %	34.03 ± 5.11	11.38 ± 1.95***	14.56 ± 1.93***
Liver TG pool, μmol/liver	23.98 ± 3.69	51.27 ± 6.15**	40.52 ± 4.58*
Absolute contribution to liver TG pool, μmol/liver	6.88 ± 1.12	5.10 ± 0.87	5.83 ± 0.93
Fractional contribution to plasma TG pool, %	39.55 ± 5.25	28.80 ± 4.30	23.77 ± 5.23
Plasma TG pool size, μmol	0.67 ± 0.05	0.67 ± 0.06	0.46 ± 0.3*/†
Absolute contribution to plasma TG pool, μmol	0.26 ± 0.04	0.19 ± 0.04	0.11 ± 0.03*

Data are means ± SE, analyzed by 1-way ANOVA with Tukey's post hoc tests where appropriate. *$P < 0.05$, **$P < 0.01$, and ***$P < 0.001$ vs. CS; †$P < 0.05$ vs. CDD; n = 12–15/group.

RESULTS

Body Composition and Liver TGs

Consistent with previous studies (37, 39), mice on MCDD lost weight (Fig. 1), with marked loss of both subcutaneous and epididymal fat (Table 2). CDD mice gained weight but less than mice on control diet (Fig. 1). Food intake (measured in the DNL study) was reduced on MCDD compared with both control diet and CDD. However, mice were otherwise active and healthy, displaying no external signs of distress.

Liver TG pool size was variable but similarly increased in both CDD and MCDD mice compared with controls after 2 wk of dietary intervention (Table 2).

Hepatic Inflammation

Steatohepatitis was confirmed in the MCDD mice, with substantially increased plasma alanine aminotransferase (Table 2) and inflammatory infiltrate in the liver on immunohistochemistry (Fig. 2). In contrast, there was no elevation in plasma transaminases or liver inflammatory infiltrate in CDD mice.

Fatty Acid Flux

Despite the loss of peripheral fat depots in the MCDD group, the R_a of palmitate did not differ between the three groups (Table 3). In keeping with this, fasting FFAs were not statistically different: 670 ± 62 vs. 602 ± 91 vs. 887 ± 220 μmol/l for CS, CDD, and MCDD, respectively.

The contribution of FFAs to TG pools was assessed in liver and plasma. Despite marked differences in the fractional contribution of plasma palmitate to liver TGs, there was no effect of diet on the absolute contribution of plasma palmitate to the liver triglyceride-derived palmitate pool. However, the contribution of plasma palmitate to circulating TG palmitate was reduced in MCDD mice.

DNL

MIDA of TG palmitate following ingestion of [$^{13}C_2$]acetate is summarized in Table 4. There were no differences in fractional synthesis rates, i.e., the percentage of newly synthesized fatty acids contributing to the TG pool, between diets. However, taking into account the differing hepatic TG pool sizes, there was a marked increase in absolute rates of hepatic DNL in MCDD mice, which was not detected in CDD mice. To investigate the molecular basis for altered DNL, we undertook real-time PCR analysis of mRNA levels in liver (Table 5). However, mRNA levels for genes involved in DNL, acetyl-CoA carboxylase-1 (ACC1), and fatty acid synthase (FAS) were not altered in MCDD mice and were paradoxically elevated in CDD mice. Moreover, mRNA levels for the principal regulator of DNL, sterol regulatory element-binding protein-1c (SREBP-1c), were suppressed in MCDD mice.

Despite increased hepatic DNL in MCDD mice, a smaller amount of newly synthesized fatty acids appeared in the plasma TG pool.

Table 4. *Effect of choline ± methionine deficiency on hepatic de novo lipogenesis and newly synthesized hepatic fatty acid export*

	CS	CDD	MCDD
Liver			
Acetyl CoA enrichment, %	7.6 ± 0.6	8.9 ± 0.5	7.2 ± 0.3
Liver TG pool, μmol/liver	25.0 ± 2.3	38.2 ± 4.0	48.5 ± 5.0**
M + 2 enrichment	0.104 ± 0.009	0.121 ± 0.008	0.132 ± 0.007
M + 4 enrichment	0.029 ± 0.003	0.041 ± 0.003*	0.036 ± 0.003
Fractional synthesis rate, %/day	5.6 ± 0.7	5.9 ± 0.4	6.8 ± 0.3
Absolute synthesis rate, μmol/day	1.4 ± 0.3	2.3 ± 0.4	3.4 ± 0.4**
Plasma TG			
Acetyl-CoA enrichment, %	7.6 ± 0.5	8.9 ± 0.4	7.4 ± 0.4
TG pool, μmol	1.7 ± 0.3	1.5 ± 0.2	1.0 ± 0.1*
Fractional synthesis rate, %/day	6.5 ± 0.5	6.2 ± 0.4	6.6 ± 0.7
Absolute synthesis rate, μmol/day	0.33 ± 0.05	0.27 ± 0.04	0.19 ± 0.03*

Results are means ± SE, analyzed by 1-way ANOVA with Tukey's post hoc tests where appropriate. Absolute synthesis rates were calculated from mass isotopomer distribution analysis of TG-derived palmitate following dietary [$^{13}C_2$]acetate labeling. The absolute synthesis rate of plasma TGs represents the hepatic export of newly synthesized fatty acids. *$P < 0.05$, **$P < 0.01$ vs. CS; n = 8/group, except for plasma TG data, where n = 5–7/group.

Table 5. *Effect of choline ± methionine deficiency on mRNA levels in liver for genes involved in de novo lipogenesis*

Gene	Genbank Reference Sequence	CS	CDD	MCDD
FAS	NM_07988.3	5.98 ± 2.47	30.64 ± 8.46**†††	0.73 ± 0.16
ACC1	NM_133360.2	7.72 ± 1.10	2.14 ± 0.63***††	5.41 ± 1.02
SREBP-1c	NM_011480.1	9.02 ± 2.22	5.21 ± 1.46	3.18 ± 0.88*

Data are expressed as means ± SE and analyzed by 1-way ANOVA with Tukey's post hoc comparison test where appropriate; $n = 5–8$/group. Results are expressed relative to internal control genes. FAS, fatty acid synthase; ACC1, acetyl-CoA carboxylase; SREBP-1c; sterol regulatory element-binding protein-1c. $*P < 0.05$, $**P < 0.01$, and $***P < 0.001$ vs. CS; $††P < 0.01$ and $†††P < 0.01$ vs. MCDD.

TG Export

Intravenous tyloxapol induced a linear increase in plasma TG levels that was not altered in CDD mice but was markedly reduced in MCDD mice (Fig. 3).

DISCUSSION

These data reveal marked differences in fatty acid metabolism in mice fed MCDD vs. CDD, which may promote the development of hepatocyte damage and steatohepatitis in the MCDD but not CDD model at similar levels of total liver triglyceride accumulation. Measurement of plasma triglycerides after tyloxapol confirmed impaired hepatic triglyceride export in the MCDD mice only, with palmitate and acetate tracer administration demonstrating that export of both newly synthesized and plasma-derived reesterified FFAs is impaired. Reduced liver secretion of fatty acids (in VLDL), and hence, supply to adipose tissue, rather than increased lipolysis and adipose release of fatty acids, may therefore contribute to loss of body fat in MCDD mice. In addition, hepatic DNL is increased in MCDD mice, potentially exacerbating accumulation of fatty acids as well as triglycerides in hepatocytes. In contrast, in choline deficiency without methionine deficiency (CDD) there were no significant changes in liver triglyceride secretion, fatty acid turnover, or DNL. No increased fatty acid esterification was measured in CDD mice by [$^{13}C_4$] dilution, as hypothesized previously (36), although we cannot exclude that a coexisting intrahepatic fatty acid pool that is not successfully labeled exists in our tracer studies and contributes to triglyceride accrual.

Both methionine and choline are key nutrients necessary for the synthesis of phosphatidyl choline and export of VLDL from the liver (27, 46). It has been widely assumed that hepatic triglyceride accumulation in both CDD and MCDD is the result of impaired VLDL export (reviewed in Ref. 22). Impaired VLDL export has recently been confirmed using tyloxapol in MCDD mice (37). However, in CDD mice this explanation is based on an experiment that demonstrated reduced incorporation of radiolabeled palmitate tracer into plasma triglycerides and retention of radioactivity in the liver in rats acutely (15 h) after a CDD was introduced (29). These observations could be explained by increased dilution of tracer in the expanded triglyceride storage pool in liver from which VLDL is exported or increased mitochondrial oxidation of palmitate and release of radioactivity. Here, we show that CDD mice studied after 2 wk of dietary manipulation do not share an impairment of hepatic VLDL export with MCDD mice. Not only was triglyceride accumulation following tyloxapol normal in CDD mice, but incorporation of palmitate tracer into plasma triglycerides was intact following tracer palmitate or acetate administration. This conclusion is supported by recent in vitro studies in mouse liver cell lines (22).

The difference in VLDL export between CDD and MCDD alone is unlikely to explain the contrasting risk of steatohepatitis. Both apolipoprotein B100 and the Mttp-encoded microsomal triglyceride transfer protein are essential for hepatic triglyceride export, and deficiency of these proteins in both mice and humans leads to hepatic steatosis (3, 26, 35, 41, 44) but critically is not associated with the inflammation seen in the MCDD model. However, impaired VLDL export may sensitize

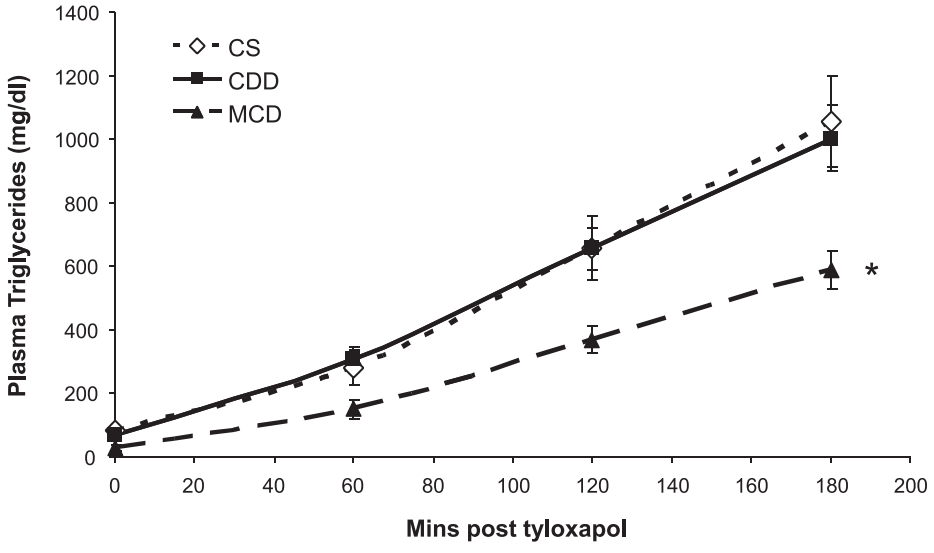

Fig. 3. Effect of methionine ± choline deficiency on plasma triglycerides following intravenous tyloxapol. Hepatic triglyceride export was reduced in the MCDD group only. Data are expressed as means ± SE. Rate of triglyceride export (142 ± 21 vs. 122 ± 15 vs. 80 ± 7 mg·kg^{-1}·h^{-1} for CS, CDD, and MCDD, respectively) was calculated from the linear portion of the graphs using *Eq. 6* and analyzed by 1-way ANOVA with Tukey's post hoc comparison test where appropriate; $n = 7–8$/group. $*P < 0.05$ vs. CS.

the liver to additional toxic insults, as evidenced by an increase in lipopolysaccharide-induced inflammation in mice with reduced hepatic Mttp expression (5). Moreover, limited circumstantial evidence suggests that patients with steatohepatitis have impaired apolipoprotein B-dependent triglyceride export (43) and more frequent polymorphisms in the Mttp gene (42).

The impaired hepatic triglyceride export and steatosis found in the apoB-38.9 mouse model of familial hypo-β-lipoproteinemia is associated with suppression of DNL, perhaps reflecting an adaptive mechanism (28). Using deuterium as a tracer, DNL has previously been shown to be lower in C3H/HeOuJ mice fed a high-sucrose lipogenic MCDD than in mice fed a methionine/choline-supplemented lipogenic diet; however, in keeping with our findings, absolute DNL rates were still markedly elevated on the lipogenic MCDD diet compared with standard chow fed controls (39). DNL has not previously been investigated in CDD mice using in vivo tracer techniques. We found that DNL is markedly increased in MCDD mice but not in CDD mice, although this result should be interpreted with the caveat that the absolute synthesis rate calculation is dependent on the hepatic triglyceride pool size, which surprisingly was not significantly increased in the CDD group in the DNL experiment (Table 4). The difference in DNL between CDD and MCDD mice was also not statistically significant. We opted to use a doubly labeled acetate tracer to improve accuracy of GC-MS for MIDA, as suggested by Chinkes et al. (7), although due to theoretical concerns over intrahepatic acetyl-CoA gradients, the use of an acetate tracer may have slightly underestimated DNL (2). Of note, we did not find that in vivo changes in DNL were reflected in corresponding changes in mRNA for ACC1 and FAS. This emphasizes the importance of performing detailed in vivo metabolic studies; it is well documented that the expression of single genes does not necessarily translate to flux through complex metabolic pathways in vivo (16). The changes in mRNA levels may be compensatory, e.g., if FAS is upregulated to compensate for the downregulation of ACC1 in CDD mice and if the downregulation of SREBP-1c in MCDD mice, as documented previously (37), serves to "restrain" FAS and ACC1 expression in the face of enhanced DNL.

It does not appear that alterations in fatty acid supply to the liver from peripheral tissues is important in the MCDD or CDD model. We studied mice after 2 wk of dietary manipulation when the fatty liver phenotypes were established. Weight loss in the MCDD mice was rapid initially and slowing by 2 wk (Fig. 1). Therefore, it is possible that we have underestimated any acute increase in peripheral fatty acid release. However, increased peripheral fat turnover does not appear necessary to maintain steatohepatitis. There is also debate as to whether the R_a of palmitate should be expressed relative to fat mass, fat-free mass, or total body weight (21). We expressed the R_a of palmitate per unit of body mass to best represent the total flux of fatty acids to the liver, although clearly the R_a of palmitate would be higher in the MCDD group if expressed relative to fat mass.

We have not made in vivo measurements of hepatic fatty acid oxidation. These are difficult, particularly in mice. Even if we had collected expired carbon dioxide or conducted indirect calorimetry (1), this would not have been specific to hepatic mitochondrial oxidation. Whole body β-oxidation rates have been shown to be elevated in MCDD mice, with an associated increase in carnitine palmitoyltransferase IA activity and palmitate oxidation measured ex vivo (39), although this was not sufficient to increase plasma β-hydroxybutyrate levels (37) or compensate for the increased hepatic fatty acid load secondary to impaired VLDL export and increased DNL. There is accruing evidence that fatty acid oxidation may be less efficient in the MCDD model (40), leading to increased microsomal and peroxisomal oxidation, generating reactive oxygen species and lipid peroxides thought to be important in the pathogenesis of inflammation and liver cell necrosis (23). Clearly, the impact in the liver of increased FFA generation and impaired export, as we have described here, would be exacerbated by any relative failure of fatty acid oxidation (15). Another technical limitation is that repeated sampling is not possible in mice to confirm that steady state of tracer enrichments has been achieved. This may be most relevant to the incorporation of labeled palmitate within triglyceride pools, although even if steady state has not been achieved, then the index we used in *Eq. 2* is likely to reliably reflect the rate of change. Finally, it would be ideal to conduct pair-feeding experiments to match weight loss in CDD and MCDD mice, although such is the severity of weight loss in MCDD mice that this would be technically very challenging.

In summary, using a number of methodologies, including in vivo tracer techniques, we have demonstrated important differences in fatty acid metabolism that associate with contrasting susceptibility to steatohepatitis in CDD and MCDD mice. We speculate that the combination of abnormalities in fatty acid metabolism in MCDD mice leads to accumulation of FFAs within the liver that is disproportionate to the accumulation of triglycerides and predisposes MCDD mice to complications. It will be important to establish whether similar changes in fatty acid metabolism are predictive of steatohepatitis and liver damage in other circumstances, including in humans.

ACKNOWLEDGMENTS

We are grateful to the Mass Spectrometry Core Laboratory of the Wellcome Trust Clinical Research Facility in Edinburgh, UK, for support. We thank Forbes Howie for help in analyzing plasma biochemistry.

GRANTS

This work was funded by the Wellcome Trust and British Heart Foundation.

DISCLOSURES

The authors have nothing to disclose.

REFERENCES

1. **Baar RA, Dingfelder CS, Smith LA, Bernlohr DA, Wu C, Lange AJ, Parks EJ.** Investigation of in vivo fatty acid metabolism in AFABP/aP2$^{-/-}$ mice. *Am J Physiol Endocrinol Metab* 288: E187–E193, 2005.
2. **Bederman IR, Reszko AE, Kasumov T, David F, Wasserman DH, Kelleher JK, Brunengraber H.** Zonation of labeling of lipogenic acetyl-CoA across the liver: implications for studies of lipogenesis by mass isotopomer analysis. *J Biol Chem* 279: 43207–43216, 2004.
3. **Björkegren J, Beigneux A, Bergo MO, Maher JJ, Young SG.** Blocking the secretion of hepatic very low density lipoproteins renders the liver more susceptible to toxin-induced injury. *J Biol Chem* 277: 5476–5483, 2002.
4. **Burdge GC, Wright P, Jones AE, Wootton SA.** A method for separation of phosphatidylcholine, triacylglycerol, non-esterified fatty acids and cholesterol esters from plasma by solid-phase extraction. *Br J Nutr* 84: 781–787, 2000.
5. **Charlton M, Sreekumar R, Rasmussen D, Lindor K, Nair KS.** Apolipoprotein synthesis in nonalcoholic steatohepatitis. *Hepatology* 35: 898–904, 2002.

6. **Chen X, Iqbal N, Boden G.** The effects of free fatty acids on gluconeogenesis and glycogenolysis in normal subjects. *J Clin Invest* 103: 365–372, 1999.
7. **Chinkes DL, Aarsland A, Rosenblatt J, Wolfe RR.** Comparison of mass isotopomer dilution methods used to compute VLDL production in vivo. *Am J Physiol Endocrinol Metab* 271: E373–E383, 1996.
8. **Donnelly KL, Smith CI, Schwarzenberg SJ, Jessurun J, Boldt MD, Parks EJ.** Sources of fatty acids stored in liver and secreted via lipoproteins in patients with nonalcoholic fatty liver disease. *J Clin Invest* 115: 1343–1351, 2005.
9. **Fabbrini E, deHaseth D, Deivanayagam S, Mohammed BS, Vitola BE, Klein S.** Alterations in fatty acid kinetics in obese adolescents with increased intrahepatic triglyceride content. *Obesity (Silver Spring)* 17: 25–29, 2009.
10. **Fabbrini E, Mohammed BS, Magkos F, Korenblat KM, Patterson BW, Klein S.** Alterations in adipose tissue and hepatic lipid kinetics in obese men and women with nonalcoholic fatty liver disease. *Gastroenterology* 134: 424–431, 2008.
11. **Feldstein AE, Canbay A, Guicciardi ME, Higuchi H, Bronk SF, Gores GJ.** Diet associated hepatic steatosis sensitizes to Fas mediated liver injury in mice. *J Hepatol* 39: 978–983, 2003.
12. **Feldstein AE, Werneburg NW, Canbay A, Guicciardi ME, Bronk SF, Rydzewski R, Burgart LJ, Gores GJ.** Free fatty acids promote hepatic lipotoxicity by stimulating TNF-alpha expression via a lysosomal pathway. *Hepatology* 40: 185–194, 2004.
13. **Folch J, Lees M, Sloane Stanley GH.** A simple method for the isolation and purification of total lipides from animal tissues. *J Biol Chem* 226: 497–509, 1957.
14. **Frayn KN.** Calculation of substrate oxidation rates in vivo from gaseous exchange. *J Appl Physiol* 55: 628–634, 1983.
15. **Ghoshal AK, Farber E.** Choline deficiency, lipotrope deficiency and the development of liver disease including liver cancer: a new perspective. *Lab Invest* 68: 255–260, 1993.
16. **Hellerstein MK.** New stable isotope-mass spectrometric techniques for measuring fluxes through intact metabolic pathways in mammalian systems: introduction of moving pictures into functional genomics and biochemical phenotyping. *Metab Eng* 6: 85–100, 2004.
17. **Hellerstein MK, Neese RA.** Mass isotopomer distribution analysis at eight years: theoretical, analytic, and experimental considerations. *Am J Physiol Endocrinol Metab* 276: E1146–E1170, 1999.
18. **Huang W, Dedousis N, Bandi A, Lopaschuk GD, O'Doherty RM.** Liver triglyceride secretion and lipid oxidative metabolism are rapidly altered by leptin in vivo. *Endocrinology* 147: 1480–1487, 2006.
19. **Itani SI, Ruderman NB, Schmieder F, Boden G.** Lipid-induced insulin resistance in human muscle is associated with changes in diacylglycerol, protein kinase C, and IkappaB-alpha. *Diabetes* 51: 2005–2011, 2002.
20. **Jung HR, Turner SM, Neese RA, Young SG, Hellerstein MK.** Metabolic adaptations to dietary fat malabsorption in chylomicron-deficient mice. *Biochem J* 343: 473–478, 1999.
21. **Koutsari C, Jensen MD.** Thematic review series: patient-oriented research. Free fatty acid metabolism in human obesity. *J Lipid Res* 47: 1643–1650, 2006.
22. **Kulinski A, Vance DE, Vance JE.** A choline-deficient diet in mice inhibits neither the CDP-choline pathway for phosphatidylcholine synthesis in hepatocytes nor apolipoprotein B secretion. *J Biol Chem* 279: 23916–23924, 2004.
23. **Leclercq IA, Farrell GC, Field J, Bell DR, Gonzalez FJ, Robertson GR.** CYP2E1 and CYP4A as microsomal catalysts of lipid peroxides in murine nonalcoholic steatohepatitis. *J Clin Invest* 105: 1067–1075, 2000.
24. **Leclercq IA, Lebrun VA, Starkel P, Horsmans YJ.** Intrahepatic insulin resistance in a murine model of steatohepatitis: effect of PPARgamma agonist pioglitazone. *Lab Invest* 87: 56–65, 2007.
25. **Lewis GF, Uffelman KD, Szeto LW, Weller B, Steiner G.** Interaction between free fatty acids and insulin in the acute control of very low density lipoprotein production in humans. *J Clin Invest* 95: 158–166, 1995.
26. **Li X, Grundy SM, Patel SB.** Obesity in db and ob animals leads to impaired hepatic very low density lipoprotein secretion and differential secretion of apolipoprotein B-48 and B-100. *J Lipid Res* 38: 1277–1288, 1997.
27. **Li Z, Vance DE.** Phosphatidylcholine and choline homeostasis. *J Lipid Res* 49: 1187–1194, 2008.
28. **Lin X, Schonfeld G, Yue P, Chen Z.** Hepatic fatty acid synthesis is suppressed in mice with fatty livers due to targeted apolipoprotein B38.9 mutation. *Arterioscler Thromb Vasc Biol* 22: 476–482, 2002.
29. **Lombardi B, Pani P, Schlunk FF.** Choline-deficiency fatty liver: impaired release of hepatic triglycerides. *J Lipid Res* 9: 437–446, 1968.
30. **Malhi H, Bronk SF, Werneburg NW, Gores GJ.** Free fatty acids induce JNK-dependent hepatocyte lipoapoptosis. *J Biol Chem* 281: 12093–12101, 2006.
31. **Matteoni CA, Younossi ZM, Gramlich T, Boparai N, Liu YC, McCullough AJ.** Nonalcoholic fatty liver disease: a spectrum of clinical and pathological severity. *Gastroenterology* 116: 1413–1419, 1999.
32. **Nakae D.** Endogenous liver carcinogenesis in the rat. *Pathol Int* 49: 1028–1042, 1999.
33. **Patterson BW, Zhao G, Elias N, Hachey DL, Klein S.** Validation of a new procedure to determine plasma fatty acid concentration and isotopic enrichment. *J Lipid Res* 40: 2118–2124, 1999.
34. **Patterson BW, Zhao G, Klein S.** Improved accuracy and precision of gas chromatography/mass spectrometry measurements for metabolic tracers. *Metabolism* 47: 706–712, 1998.
35. **Raabe M, Véniant MM, Sullivan MA, Zlot CH, Björkegren J, Nielsen LB, Wong JS, Hamilton RL, Young SG.** Analysis of the role of microsomal triglyceride transfer protein in the liver of tissue-specific knockout mice. *J Clin Invest* 103: 1287–1298, 1999.
36. **Raubenheimer PJ, Nyirenda MJ, Walker BR.** A choline-deficient diet exacerbates fatty liver but attenuates insulin resistance and glucose intolerance in mice fed a high-fat diet. *Diabetes* 55: 2015–2020, 2006.
37. **Rinella ME, Elias MS, Smolak RR, Fu T, Borensztajn J, Green RM.** Mechanisms of hepatic steatosis in mice fed a lipogenic methionine choline-deficient diet. *J Lipid Res* 49: 1068–1076, 2008.
38. **Rinella ME, Green RM.** The methionine-choline deficient dietary model of steatohepatitis does not exhibit insulin resistance. *J Hepatol* 40: 47–51, 2004.
39. **Rizki G, Arnaboldi L, Gabrielli B, Yan J, Lee GS, Ng RK, Turner SM, Badger TM, Pitas RE, Maher JJ.** Mice fed a lipogenic methionine-choline-deficient diet develop hypermetabolism coincident with hepatic suppression of SCD-1. *J Lipid Res* 47: 2280–2290, 2006.
40. **Romestaing C, Piquet MA, Letexier D, Rey B, Mourier A, Servais S, Belouze M, Rouleau V, Dautresme M, Ollivier I, Favier R, Rigoulet M, Duchamp C, Sibille B.** Mitochondrial adaptations to steatohepatitis induced by a methionine- and choline-deficient diet. *Am J Physiol Endocrinol Metab* 294: E110–E119, 2008.
41. **Schonfeld G, Patterson BW, Yablonskiy DA, Tanoli TS, Averna M, Elias N, Yue P, Ackerman J.** Fatty liver in familial hypobetalipoproteinemia: triglyceride assembly into VLDL particles is affected by the extent of hepatic steatosis. *J Lipid Res* 44: 470–478, 2003.
42. **Schonfeld G, Yue P, Lin X, Chen Z.** Fatty liver and insulin resistance: not always linked. *Trans Am Clin Climatol Assoc* 119: 217–223, 2008.
43. **Tietge UJ, Bakillah A, Maugeais C, Tsukamoto K, Hussain M, Rader DJ.** Hepatic overexpression of microsomal triglyceride transfer protein (MTP) results in increased in vivo secretion of VLDL triglycerides and apolipoprotein B. *J Lipid Res* 40: 2134–2139, 1999.
44. **Wetterau JR, Aggerbeck LP, Bouma ME, Eisenberg C, Munck A, Hermier M, Schmitz J, Gay G, Rader DJ, Gregg RE.** Absence of microsomal triglyceride transfer protein in individuals with abetalipoproteinemia. *Science* 258: 999–1001, 1992.
45. **Yamaguchi K, Yang L, McCall S, Huang J, Yu XX, Pandey SK, Bhanot S, Monia BP, Li YX, Diehl AM.** Inhibiting triglyceride synthesis improves hepatic steatosis but exacerbates liver damage and fibrosis in obese mice with nonalcoholic steatohepatitis. *Hepatology* 45: 1366–1374, 2007.
46. **Zeisel SH, Blusztajn JK.** Choline and human nutrition. *Annu Rev Nutr* 14: 269–296, 1994.